This document was prepared in conjunction with work accomplished under Contract No. DE-AC09-96SR18500 with the U. S. Department of Energy.

DISCLAIMER

This report was prepared as an account of work sponsored by an agency of the United States Government. Neither the United States Government nor any agency thereof, nor any of their employees, nor any of their contractors, subcontractors or their employees, makes any warranty, express or implied, or assumes any legal liability or responsibility for the accuracy, completeness, or any third party's use or the results of such use of any information, apparatus, product, or process disclosed, or represents that its use would not infringe privately owned rights. Reference herein to any specific commercial product, process, or service by trade name, trademark, manufacturer, or otherwise, does not necessarily constitute or imply its endorsement, recommendation, or favoring by the United States Government or any agency thereof or its contractors or subcontractors. The views and opinions of authors expressed herein do not necessarily state or reflect those of the United States Government or any agency thereof.

CONTAINMENT EVALUATION OF BREACHED AL-SNF FOR CASK TRANSPORT

D.W. Vinson, R.L. Sindelar, and N.C. Iyer
Savannah River National Laboratory - Materials Science & Technology
Aiken, SC 29808 – USA

ABSTRACT

Aluminum-based spent nuclear fuel (Al-SNF) from foreign and domestic research reactors (FRR/DRR) is being shipped to the Savannah River Site. To enter the U.S., the cask with loaded fuel must be certified to comply with the requirements in the Title 10 of the U.S. Code of Federal Regulations, Part 71. The requirements include demonstration of containment of the cask with its contents under normal and accident conditions. Al-SNF is subject to corrosion degradation in water storage, and many of the fuel assemblies are "failed" or have through-clad damage. A methodology has been developed with technical bases to show that Al-SNF with cladding breaches can be directly transported in standard casks and maintained within the allowable release rates. The approach to evaluate the limiting allowable leakage rate, L_R, for a cask with breached Al-SNF for comparison to its test leakage rate could be extended to other nuclear material systems.

The approach for containment analysis of Al-SNF follows calculations for commercial spent fuel as provided in NUREG/CR-6487 that adopts ANSI N14.5 as a methodology for containment analysis. The material-specific features and characteristics of damaged Al-SNF (fuel materials, fabrication techniques, microstructure, radionuclide inventory, and vapor corrosion rates) that were derived from literature sources and/or developed in laboratory testing are applied to generate the four containment source terms that yield four separate cask cavity activity densities; namely, those from fines; gaseous fission product species; volatile fission product species; and fuel assembly crud. The activity values, A_2, are developed per the guidance of 10CFR71. The analysis is performed parametrically to evaluate maximum number of breached assemblies and exposed fuel area for a proposed shipment in a cask with a test leakage rate.

Introduction

Foreign and domestic research reactor spent nuclear fuel is being shipped to SRS under the site FRR/DRR Receipts Program. The cladding of a small percentage of this fuel has been breached due to corrosion or mechanical damage [6]. Fuel with minor breaches can be directly stored in the SRS basins because of the expected low release levels of radioactivity from the fuel [8].

The broad-based criteria for acceptance of the fuel includes that transportation of the fuel must comply with all Certificate of Compliance (COC) conditions for the U.S. shipping casks and Certificate of Competent Authority (CoCA) for the foreign casks. Specifically, to enter the United States, the cask needs to comply with the U. S. Code of Federal Regulations (CFRs). The requirements for transportation, contained in 10CFR71 [1], include demonstration of containment under normal and accident conditions. The NRC recognizes ANSI N14.5 [2] as an approved methodology to perform the analyses for containment. Sample calculations of containment analyses for transportation are given in NUREG/CR-6487 [3], which used ANSI N14.5 methodology.

The inputs and assumptions for commercial spent nuclear fuel are not, in general, applicable to research reactor fuel. The present document describes the bases for the assumptions and inputs that are applicable to containment analysis for shipping breached Al-SNF. .

The following source terms for containment analyses of Al-SNF during shipping are evaluated in this report:

- Fuel Fines;
- Gaseous Fission Product Species;
- Volatile Fission Product Species; and
- Fuel Assembly Crud (activity associated with the oxide layer of the cladding material).

A nomograph to evaluate the acceptability of a cask with a given standard leakage rate to contain breached Al-SNF is presented.

Part I – Containment Analysis Methodology

The approach to evaluate the radioactivity release from breached Al-SNF within a cask with a reference leak rate follows an established methodology for commercial SNF with material-specific inputs. Part I of this paper describes the containment methodology with specific inputs. Part II describes the bases for the inputs for Al-SNF. The calculations for breached Al0SNF follow NUREG/CR-6487 [3], which adopts ANSI N14.5 [2] as a methodology for containment analysis. The material-specific inputs for Al-SNF were developed from laboratory tests and analyses and literature information. The Al-SNF is typically plate assemblies of the Materials Test Reactor equivalent design. Two examples of Al-SNF are listed in Table 1.

Calculation of Permissible Leakage Rates

The containment criterion for Type B packages requires that a package have a radioactive release rate less than $A_2 x 10^{-6}$ in one hour and A_2 per week under normal conditions of transport and for accident conditions, respectively. The parameter A_2 has units of curies (Ci) and is isotope dependent. A_2 is calculated from the isotopic curie concentration in the fuel as determined through use of the SAS2h module of SCALE4.3. The assumed release fractions for the various radionuclides transported in a Type B package is summarized in Table 2.

Table 1 Input Assumptions for SAS2h

Parameter	Example Fuel #1	Example Fuel #2
Specific Power [MW]	1.07	1.472
Burn Time [days]	197	125
Cool Time [days]	365.25	730.5
Moderator	D_2O	D_2O
Moderator Temperature [K]	325	325
Clad Temperature [K]	446	446
Fuel Temperature [K]	447	447
Active Meat Thickness [cm]	0.058	0.051
Active Meat Width [cm]	5.715	6.71
Active Meat Length [cm]	57.79	60
Number of Plates	18	23
Clad Thickness [cm]	0.035	0.038
Pitch [cm]	0.381	0.345
Fuel Material Masses [g]		
U-235	351.00	450.00
U-238	26.42	33.87
O	68.46	87.77
Al	668.82	857.47

Table 2 Summary of Inputs for Al-SNF to Example Release Calculations

Parameter	Normal Conditions of Transport	Hypothetical Accident Conditions
Fraction of Breached Fuel in a Cask, f_b This is the fraction of assemblies in a cask that could release gas, volatiles, and that result in fuel surface area exposure.	0.10	1.00
Fission Gas Release Fraction, f_G	0.30	1.00
Volatile Release Fraction, f_V	1E-06	1E-06
Meat Surface Area Exposed, ESA. This can be applied on a per-assembly or a per-cask basis.	1% of outside plates (e.g., 27.8 cm^2 for Example Cask #1)	1% of outside plates (e.g., 27.8 cm^2 for Example Cask #1)
Fraction of Fuel Meat Corrosion Product Layer Released due to Spallation, T_F	0.15	1.00
Crud Spallation Fraction, f_C	0.15	1.00

Assuming that the release rate is independent of time, the maximum permissible release rates for normal (R_N) and accident (R_A) conditions of transport, respectively, can be expressed as follows:

$R_N = L_N C_N \leq A_{2,N} \times 2.78 \times 10^{-10}$ /second, (Eq. 1)
$R_A = L_A C_A \leq A_{2,A} \times 1.65 \times 10^{-6}$ /second, (Eq. 2)

where:

R_i is the release rate for normal (R_N) and accident (R_A) conditions of transport [Ci/s],
L_i is the volumetric gas leakage rate [cm^3/s] under normal (L_N) and accident (L_A) conditions of transport,
C_i is the curies per unit volume of the radioactive material, "activity density", that passes through the leak path for normal (C_N) and accident (C_A) conditions of transport [Ci/cm^3], and
$A_{2,i}$ is the mixture A_2 of the radionuclides available for release under normal $A_{2,N}$ and $A_{2,A}$ accident conditions of transport [Ci].

Additionally, for accident conditions, an effective A_2 value equal to $10 \bullet A_2$ may be used for krypton-85.

Determination of the Activity Density of Releasable Material

There are four sources of radioactive material that may become airborne during transportation. These sources are gases, volatiles, fines, and crud. The contributions to the total activity density in the shipping cask free volume from the four sources are treated separately as follows.

$C_{total} = C_{gas} + C_{vol} + C_{fines} + C_{crud}$, (Eq. 3)

where:

C_{total} is the total releasable activity density inside the containment vessel [Ci/cm^3],
C_{gas} is the releasable activity density inside the containment vessel due to the release of gas [Ci/cm^3],
C_{vol} is the releasable activity density inside the containment vessel due to the release of volatiles [Ci/cm^3],
C_{fines} is the releasable activity density inside the containment vessel due to the release of fines [Ci/cm^3], and
C_{crud} is the releasable activity density inside the containment vessel as a result of crud spallation [Ci/cm^3].

The releasable activity density [Ci/cm^3] inside the containment vessel due to the release of gas may be described by either Eq. 4or Eq. 5.

$C_{gas} = (A_G \bullet f_b \bullet f_G)/V_C$, (Eq. 4)
$C_{gas} = (A_{gb} \bullet N_b \bullet f_G)/V_C$, (Eq. 5)

where:

A_G is the total number of curies of all gaseous radionuclides in all assemblies in the cask. It is the product of the number of assemblies and the number of curies of all gaseous isotopes per assembly (i.e., as output by ORIGEN-S) [Ci],
f_b is the fraction of fuel assemblies that are breached in a cask [$f_{b,N}$=0.1, $f_{b,A}$=1.0],
f_G is the fraction of gas that escapes the breached fuel assembly [$f_{G,N}$=0.3,$f_{G,A}$=1.0],
V_C is the free volume of the cask [cm^3],
A_{gb} is the number of curies of all gaseous radionuclides in a single breached assembly (i.e., as output by ORIGEN-S) [Ci], and
N_b is the number of breached fuel assemblies in cask.

The releasable activity density [Ci/cm^3] inside the containment vessel due to the release of volatiles may be described by either Eq. 6 or Eq. 7.

$$C_{vol} = (A_V \bullet f_b \bullet f_V)/V_C, \quad \text{(Eq. 6)}$$
$$C_{vol} = (A_{vb} \bullet N_b \bullet f_V)/V_C, \quad \text{(Eq. 7)}$$

where:

A_V is the total number of curies of all volatile radionuclides in all assemblies in the cask. It is the product of the number of assemblies and the number of curies of all volatile isotopes per assembly (i.e., as output by ORIGEN-S) [Ci],
f_V is the fraction of gas that escapes the breached fuel assembly [$f_{V,N}$=$f_{V,A}$=1E-6],
A_{vb} is the number of curies of all volatile radionuclides in a single breached assembly (i.e., as output by ORIGEN-S) [Ci], and

The releasable activity density [Ci/cm^3] inside the containment vessel due to the release of fines is described by Eq. 8.

$$C_{fines} = (A_F \bullet ESA \bullet P \bullet T_F/V_M) \bullet (1/V_C), \quad \text{(Eq. 8)}$$

where:

A_F is the total number of curies of all radionuclides in all assemblies in the cask (excluding gases). It is the product of the number of assemblies and the number of curies of the all isotopes (excluding gases) per assembly (i.e., as output by ORIGEN-S) [Ci],
ESA is the amount of exposed meat surface area per cask [cm^2/cask],
P is the depth of corrosion attack [5.E-04-cm],
T_F is the oxide spallation fraction [$T_{F,N}$=0.15, $T_{F,A}$=1.0],
V_M is the volume of the meat region of the fuel per cask [cm^3/cask], and

The releasable activity density [Ci/cm^3] inside the containment vessel as a result of crud spallation is described by Eq. 9.

$$C_{crud} = (f_C \bullet S_C \bullet S_A)/V_C, \quad \text{(Eq. 9)}$$

where:

f_C is the crud spallation fraction [$f_{C,N}$=0.15, $f_{C,A}$=1.0],
S_C is the crud surface activity [1.39E-7 Ci/cm^2],
S_A is the sum of the surface areas of all assemblies [cm^2], and

The free volumes inside the containment vessel for the casks are typically on the order of 10^5 cm^3. A total of 30 to 40 MTR assemblies are typically loaded the casks.

Activity Values for Radionuclides

A_2 values for the fuel gases, volatiles, fines, and crud are derived from the values provided in Appendix A, Table A-1 of 10CFR71. The A_2 values for those isotopes for which no specific A_2 value is specified are determined using the guidance provided in the appendix. The A_2 value for mixtures of isotopes is calculated from:

$$A_2 = (\sum(R_i/A_{2i}))\text{-}1, \qquad \text{(Eq. 10)}$$

where:

R_i is the fraction activity of nuclide *i* in the mixture and
A_{2i} is the appropriate A_2 value for nuclide *i*.

A mixture A_2 is determined by Eq. 10 for gases, volatiles, fines, and crud. These mixture A_2 values are then combined using Eq. 11 to obtain a total cask mixture A_2.

$$A_2 = (\sum(F_i/A_{2i}))\text{-}1, \qquad \text{(Eq. 11)}$$

where:

F_i is the fraction activity density of contributor *i* (i.e., gas, volatiles, fines, or crud) in the mixture and
A_{2i} is the appropriate A_2 value for mixture *i* [Ci].

Determination of the Maximum Permissible Leakage Rate

The maximum permissible leak rate is calculated by using the solutions to Eq. 11 and Eq. 3 and solving for L_i in Eq. 1 and Eq. 2 at normal conditions of transport and accident conditions of transport, respectively. The values of these parameters are provided in the Tables 6 and 7 for normal conditions of transport and accident conditions, respectively.

Maximum Permissible Leakage Rate at Standard Conditions

The volumetric gas leak rate is modeled as a combination of continuum and molecular flow through a single leak path. The leak path is modeled as a smooth, right-circular cylinder with sharp edges. Based on these assumptions, the equation for gas leaking from the cask takes the following form.

$$L = L_c + L_m, \quad \text{(Eq. 12)}$$

where:

L is the volumetric gas flow rate at P_u [cm^3/sec],
L_c is the volumetric flow rate due to continuum flow [cm^3/sec], and
L_m is the volumetric flow rate due to molecular flow [cm^3/sec].

The volumetric flow rate, Lc, for continuum flow is given by

$$L_c = [(2.49x10^6 D^4)/a\mu] \bullet (P_u - P_d)(P_a/P_u) = F_c(P_u - P_d)(P_a/P_u), \quad \text{(Eq. 13)}$$

where:

F_c is the continuum flow coefficient [cm^3/s],
D is the capillary diameter [cm],
a is the capillary length [cm] (typically found in the SAR of a given cask),
μ is the fluid viscosity [cP] (typically found in CRC Handbook),
P_u is the upstream pressure [atm] (typically found in the SAR of a given cask),
P_d is the downstream pressure [atm], and
P_a is the average pressure, $(P_u - P_d)/2$ [atm].

The volumetric flow rate, L_m, for molecular flow is given by

$$L_m = [(3.81x10^3 D^3 (T/M)^{0.5})/aP_a] \bullet (P_u - P_d)(P_a/P_u) = F_m(P_u - P_d)(P_a/P_u), \quad \text{(Eq. 14)}$$

where:

F_m is the molecular flow coefficient [cm^3/atm•s],
T is the gas temperature [K] (typically found in the SAR of a given cask), and
M is the gas molecular weight [g/mole] (typically found in CRC Handbook).

The volumetric flow rates described above are flow rates at the upstream pressure.

To correlate the maximum permissible leak rates as summarized in **Error! Reference source not found.** and **Error! Reference source not found.** to the leak rate at standard temperature and pressure, Eq. 12 is solved for the capillary diameter (see Eq. 13 and Eq. 14) at the expected environmental conditions. The resulting diameter is then used in Eq. 12 with the temperature equal to 298-K, the upstream and downstream pressures equal to 1.0 atm and 0.01 atm, respectively, and the gas molecular weight and viscosity equal to that of dry air at standard temperature and pressure.

Part II – Mechanistic Bases for Input Assumptions

Basis for Damaged Fuel Fraction and Exposed Surface Area

Most of the SNF assemblies from research reactors are being stored in water-filled basins in the U.S. and around the world. Some of this fuel has been in water storage for longer than 35 years and the water quality, in several cases, has been aggressive to cause corrosion during some portion of this storage time. This has resulted in pitting corrosion of some of the fuel assemblies. The corrosion process results in nodular white corrosion products on the cladding surfaces of the fuel elements of the assemblies. This product can be readily observed by visual inspection of the fuel while still in the basins. Storage of fuel in a dry condition can not cause further damage unless water enters the dry storage system.

Pitting and General Corrosion of Al-SNF in Basin Storage

During reactor operation, the aluminum cladding on aluminum-based fuel develops an aluminum oxide coating, ranging from a few angstroms to several tens of μm in thickness, depending on the conditions of irradiation. The aluminum-clad fuel plates may appear grayish or off-white in color, which is due to the presence of oxide film that is protective against corrosion [9]. The aluminum oxide films are very tenacious and resistant to spallation. However, fuel handling can cause scratches in the coating, resulting in breach of the oxide and provide sites susceptible to initiation of pitting corrosion [9]. If the water chemistry is aggressive, pitting can occur. Laboratory corrosion testing has established the role of water chemistry and conductivity on pitting initiation of aluminum alloys [10].

The external surfaces of the rectangular shaped MTR fuel assembly is readily visible for inspection as the assembly is brought to within a few feet of the water surface. The two external fuel plates are the most visible and important surface areas of the visual inspection (see **Error! Reference source not found.** and Figure 1). The top edges of the internal fuel plates are visible from above the surface of the water. The two external surfaces are considered to be a conservative representation of the condition of the non-visible surfaces of the fuel assembly because:

a) Pitting corrosion is initiated when the oxide surface is breached [9]. The external plates, which surround the interior fuel plates, are most susceptible to scratches in the protective oxide coating formed during irradiation of the fuel element, resulting in a higher probably of pitting corrosion than on the interior fuel plates,

b) Impurities in the water can plate out or deposit on the aluminum to form localized anodic/cathodic sites have direct access to the external plates, whereas flow to the interior plates is lower and somewhat restricted by the geometry.

c) The external plates are the contact points for a galvanic couple between stainless steel or other dissimilar-metal storage racks and aluminum with corrosion currents highest at these contact locations. Corrosion currents are lower on the interior plates, not only because

they are further away from the contact points, but also because the current does not readily flow around a corner [11].

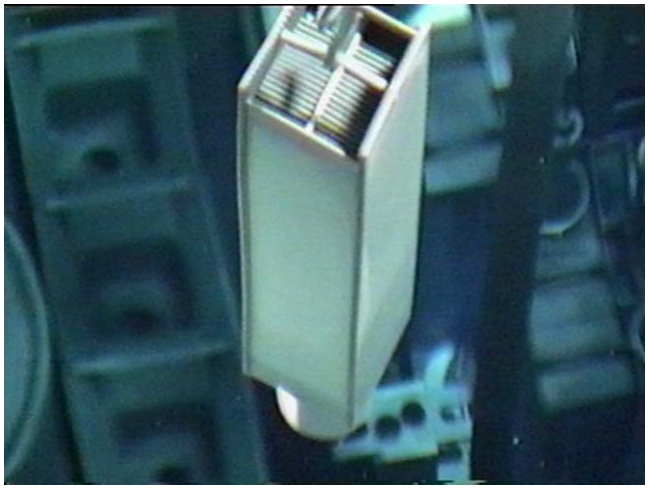

Figure 1 MTR Assembly Free of Corrosion Damage

Numerous field assessments confirm the above hypothesis. A non-irradiated MTR type fuel stored in stainless steel storage racks at the IPEN IEA-R1 Research Reactor in Brazil has shown pitting corrosion only on external fuel plates. The staff at the IPEN IEA-R1 stated that this assembly was disassembled and reassembled showed no nodular pitting on the internal plate surfaces. This has been documented in an internal IPEN report [12]. Additionally, the results of an analysis of the release of radioactivity from the IEA-R1 assemblies directly correlated to the exposed fuel meat area on the external plate surface [8]. Further SRS plant experience with production Al-U fuel and Al clad depleted U core targets also confirm that the inner fuel or target element is corrosion free even under the extreme conditions where the outer fuel or target may have had significant corrosion. Figure 2 shows an extremely corroded Al clad depleted U core outer target in comparison to corrosion free inner target. It should be noted that the extreme corrosion on the outer clad target is due to the corrosion characteristics of depleted uranium and is being presented here only to graphically show the difference in corrosion characteristics between outside and inside tubes. The Al-U SNF has different corrosion characteristics where, in the worst case, is shown in Figure 3.

Corrosion products located outside the fuel meat region of the assembly (side plates, end fittings and extremities of the fuel plates) have no potential for the release of fission products, because these locations contain no active fuel meat.

Figure 2 Mk-31 Outer and Inner Target Tubes. The tubes are aluminum-clad uranium metal.

The corrosion potential and corrosion rate of fuel meat material is similar to that of aluminum cladding in both basin-quality water chemistry [10] and aggressive water chemistry [13]. If conditions to aggressive corrosion of the fuel meat material are present, the fuel meat will dissolve and no passivating film (oxide film) will form (e.g. J-13 water chemistry) [13]. If conditions conducive to aggressive corrosion (e.g. pitting) are not present, both exposed aluminum and uranium-aluminum alloy fuel meat will form stable, passive films in waters with pH levels from approximately 4 to 10, up to moderate temperatures (100+°C). These films provide a high resistance to continued corrosion. The film thickness, f, under these conditions can be expressed as logarithmic function:

$$FilmThickness = a + b\ln(time) \qquad \text{(Eq. 15)}$$

Where the coefficients *a* and *b* are dependent on the temperature and water flow rate. Using distilled, deionized water with a conductivity of 0.71 µS /cm and low flow conditions, Draley [14] measured the weight gains and weight losses of aluminum 1100, a cladding alloy, in both low oxygen (helium-saturated water) and oxygen saturated water conditions at 50, 70, and 95°C. Basins are open to air and are oxygen-saturated. Using the data in Reference 14, approximately 1 to 2 µm of aluminum would corrode and be retained in an oxide film layer of approximately 2 to 4 µm.

Presently, the water qualities in foreign basin storage are good [6]. For this reason, exposed fuel meat should be passivated with a hydrated oxide film. An initial fuel meat thickness of 1 µm incorporated in the hydrated oxide film is applied as an initial condition for potential fines from breached fuel.

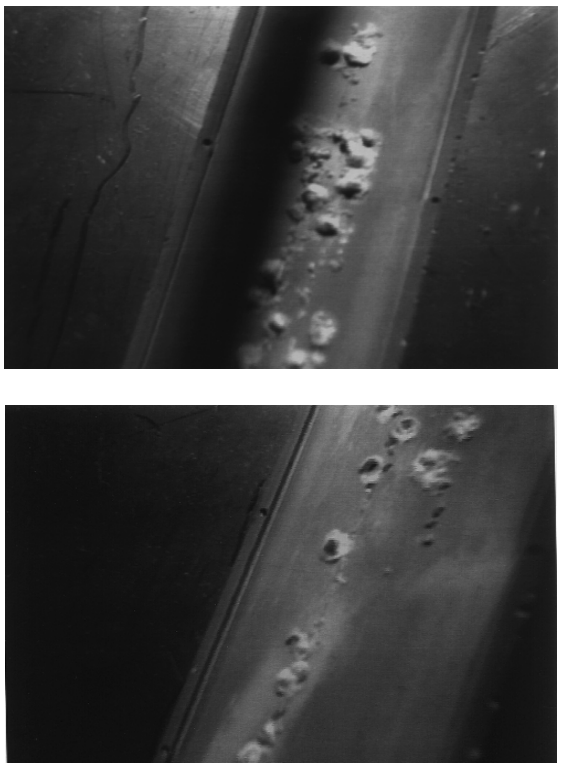

Figure 3 Nodular Pitting Corrosion on Fuel Plate of MTR Assembly Before and After Nodules Removed (Assembly IEA-53)

Basis for Through-clad Pitting Criteria for Corrosion Nodules

Corrosion nodules, if sufficiently large, are indicative of a cladding penetration on the Al-SNF assemblies. The size of a corrosion nodule at which cladding penetration has likely occurred is based on several years of corrosion surveillance testing of aluminum alloys in SRS basins and on the analysis of the underwater video of the MTR type aluminum-clad spent fuel at the IPEN-IEA-R1 Research Reactor [15]. Using underwater photography, corrosion nodules of a diameter of about 1/8 inch, or greater, are associated with a pit through the 15-mil (0.015 in) clad as judged from comparisons of drilled holes of a known diameter on the edges of the side plates. Nodules of less than 1/8 inch in diameter did not appear to have underlying pits penetrating the cladding.

Bases for the Damaged Fuel Fraction and Exposed Surface Area

Visual examination of over 1700 aluminum-clad, aluminum-based spent fuel (Al-SNF) assemblies in storage at foreign and domestic research reactor locations has shown a total of approximately 7% of the SNF assemblies to contain through-clad penetrations [6]. The majority of the breached fuels were primarily located at three storage sites, Australia, Brazil, and Thailand. The failed fuels at these sites have been considered for the purposes of this report. Excluding

these sites, approximately 2% of the fuels have cladding breaches based on the examination criteria.

Assembly IEA-53 from the IEA-R1 reactor in Brazil contains the greatest level of exposed fuel meat observed in the world-wide examinations. This fuel has been characterized as having approximately 10 pits of approximately ¼ -inch diameter or a total of 0.5 square inches (3.2 cm^2) of exposed fuel meat (see Figure 4). This corresponds to an area fraction of 1% for the one side of the fuel plate. As discussed above, the outer fuel plates are typically the only ones that should exhibit corrosion damage. Therefore in the example calculations, the assumption is made to use 1% as the exposed area of each side of each external fuel plate per assembly.

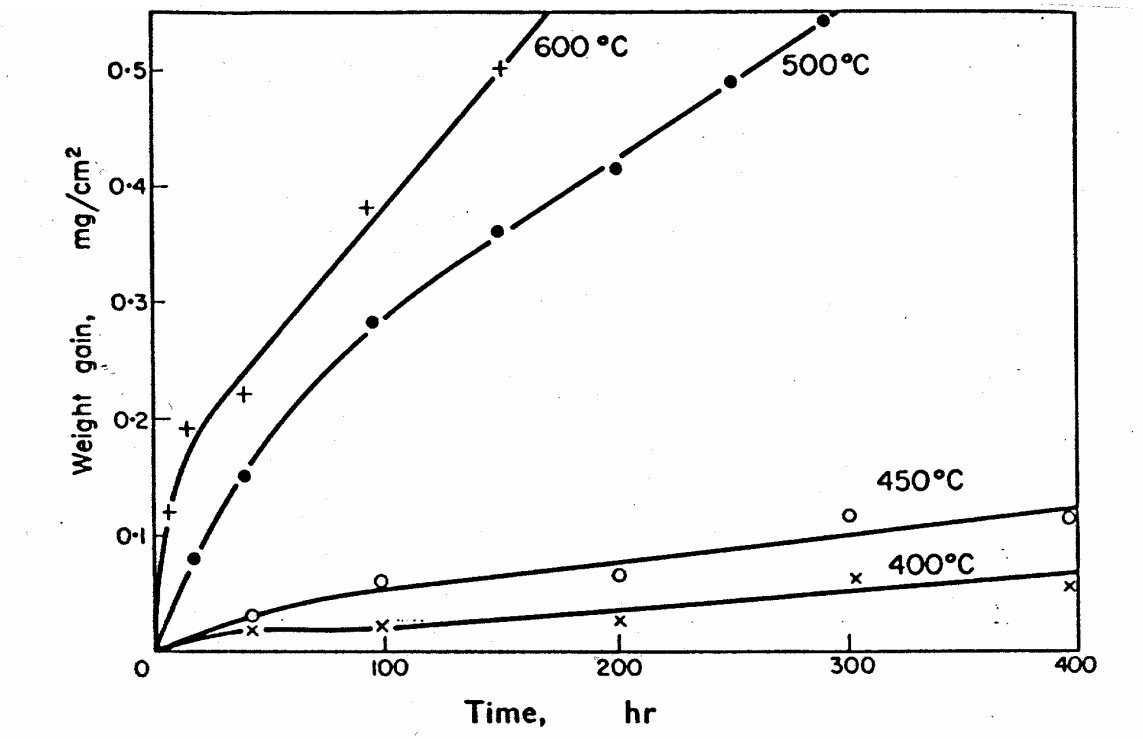

Figure 4 Weight Gain Relationship for Oxidation of 30% UAl_4-Al in the Range 400 to 600°C (reproduced from Reference 16)

Basis for Release of Fines from Exposed Fuel Meat

If a pit has penetrated the cladding in basin storage, the fuel meat would begin to corrode while in basin storage. As stated above, the corrosion of uranium-aluminum alloy materials in water is similar to aluminum metal corrosion and an initial hydrated oxide film of 2 to 4 μm incorporating a layer of 1 to 2 μm of fuel meat would be formed in high quality waters after several years storage.

The initial oxide film on the exposed fuel in dry shipping casks is subject to growth under time/temperature conditions. The resulting film is taken to be a simple summation of the passive

film thickness in water storage plus the change in thickness at the environmental conditions (after a passive film has formed at those conditions).

The kinetics of oxidation of the intermetallic compounds UAl_2, UAl_3, and UAl_4 in aluminum in dry air in the temperature range of 250 to 600°C have been studied [16]. The results from the 30% UAl_4-Al alloy are reproduced in Figure 4. An estimate of the rate of weight gain at temperatures up to 400°C for linear extrapolation is 10 μg/dm^2/hour. Assuming the oxide to be predominantly Al_2O_3, a maximum thickness of 3.7 μm of fuel meat would be corroded and retained in the oxide for a one-year exposure. For the SAR condition of <200°C (normal operation), the oxide film thickness will be <3.7 μm.

Corrosion of aluminum and uranium-aluminum alloys has been studied under wet air conditions [17]. The results show a strong dependency on relative humidity and a strong temperature dependency to alloys with an initial 600 grit finish. Subsequent exposure to a wet or dry air condition, however, results in a parabolic trend of oxide film formation. That is, the continued growth rate of a film slows as the film thickness increases.

Shipping casks are drained and shipped dry. The maximum humidity expected in the casks should be << 50% at 200°C [18]. The rate of 15 μgm/dm^2/hour is the approximate rate of weight gain on aluminum alloy materials in at 50% relative humidity vapor (RH) at 150°C at the end of several months exposure [17]. Linear extrapolation with this rate is used to estimate the weight gain after exposure for one year. Using the following correlation [17],

Metal Loss (mils) = 1.193x10^{-6} x Wt. Gain (μg/dm^2)
Oxide Film Thickness (Boehmite film in nm) = 0.0533319 x Wt. Gain (μg/dm^2),

the thickness of fuel meat within the formed hydrated oxide is 4 μm after exposure for one year. It must be noted that the formation of the oxide is time-dependent. That is, if the exposed fuel is exposed to the environmental condition 50% RH at 150°C, 4 μm of corroded fuel meat are not immediately available for release.

Exposure of U-Al alloy at saturated water vapor (100% RH) at 200°C results in a slightly greater rate of oxide film growth. Figure 5 shows that, using linear extrapolation, a rate 20 to 22 μg/dm^2/hr is observed for extruded U-Al. At 22 μg/dm^2/hr for a one-year exposure, 5.8 μm of fuel meat would be expected in the oxide film. It should be recognized however that a condition of 200°C, 100% RH is not reasonable.

A total of 5 μm of fuel meat is assumed for both normal and accident transport conditions. The fuel meat will be incorporated into the oxide layer. These assumptions are used to determine the amount of radioisotopes that are available for release as fines in the bounding case analysis of the oxide film on exposed fuel meat of aluminum-based fuel.

In reality, the oxide films formed on aluminum and uranium-aluminum are tenacious and not readily removed. Figure 6 shows a ring specimen of exposed 18U-Al before and after exposure to saturated vapor at 150°C for one year. Although it appeared blackish, Boehmite, $Al_2O_3 \cdot H_2O$, was the predominant oxide determined by x-ray diffraction analysis. It was extremely difficult

to remove (scrape) the oxide for XRD analysis. Thus, the oxide film that forms on uranium-aluminum alloys exposed to dry and wet air environments is highly adherent and not expected to dislodge unless deliberately scraped. A value of 0.15, consistent with the fraction of crud assumed to dislodge in commercial fuel, is used as the fraction of the oxide film that is removed during transport under normal conditions. A value of 1, or all of the oxide film, is assumed to dislodge during transport under accident conditions.

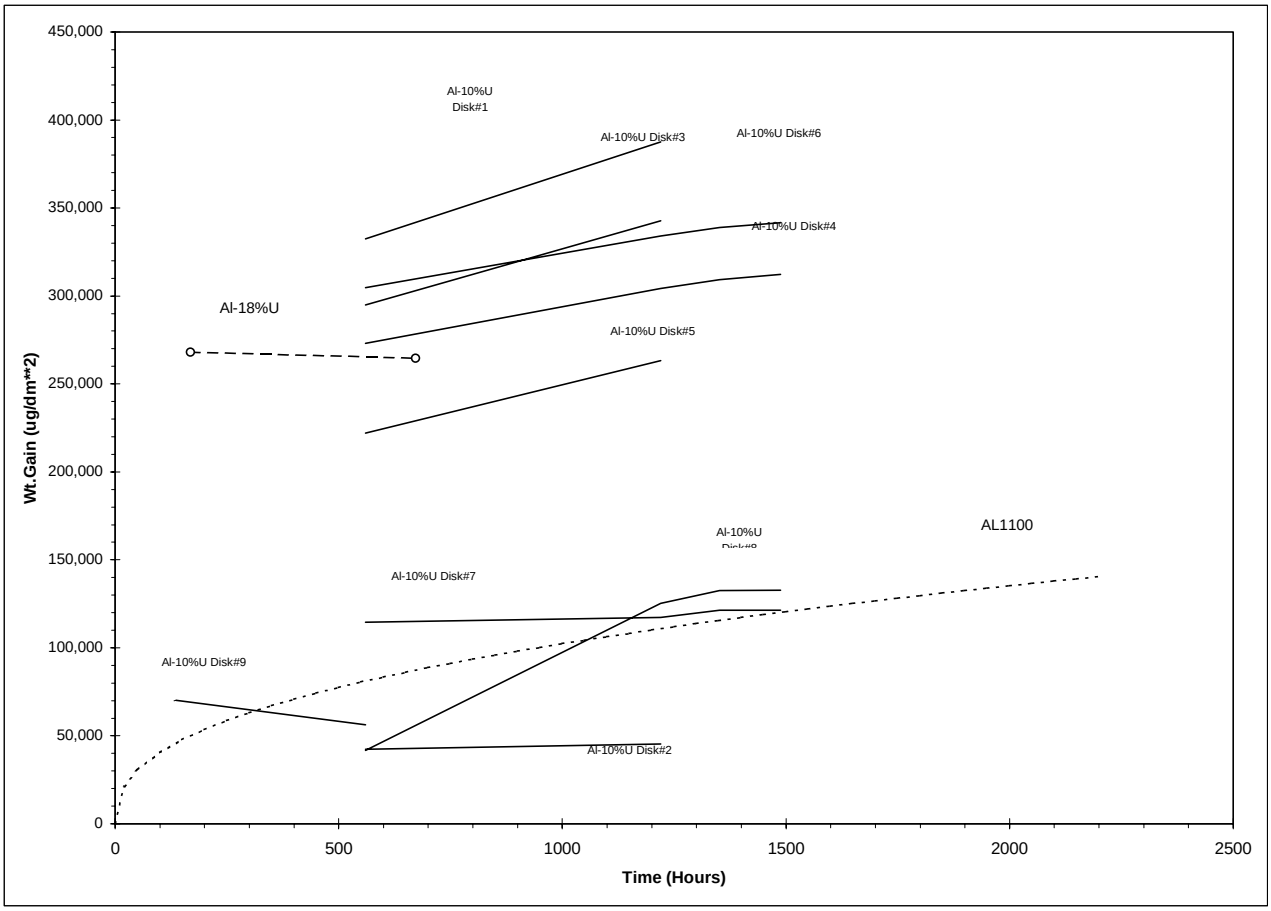

Figure 5 Weight Gain of U-Al Alloy at 200°C in Saturated Water Vapor

Gaseous and Volatile Specie Release Characteristics of Oxides on Al-SNF – Basis for Gas and Volatile Species Source Term

Gas Release

Release of gaseous species namely Kr, H^3, Xe, and I from Al-SNF are diffusion-limited (time-temperature dependent), in contrast to a direct release mechanism for commercial SNF. The gases in the aluminum SNF reside in trap sites at the defects produced during irradiation in the fuel microstructure. Transport of these gases to the exposed fuel surface involves a series of detrap/trap interactions of the solute with traps (microstructural features) in the fuel in combination with diffusion. The release of gases is therefore a function of the energy required to detrap the gases and migrate to the surface of the fuel. The energy required to detrap the gases

can be calculated through complex models while the diffusion of gases in a trap-free microstructure can be readily estimated.

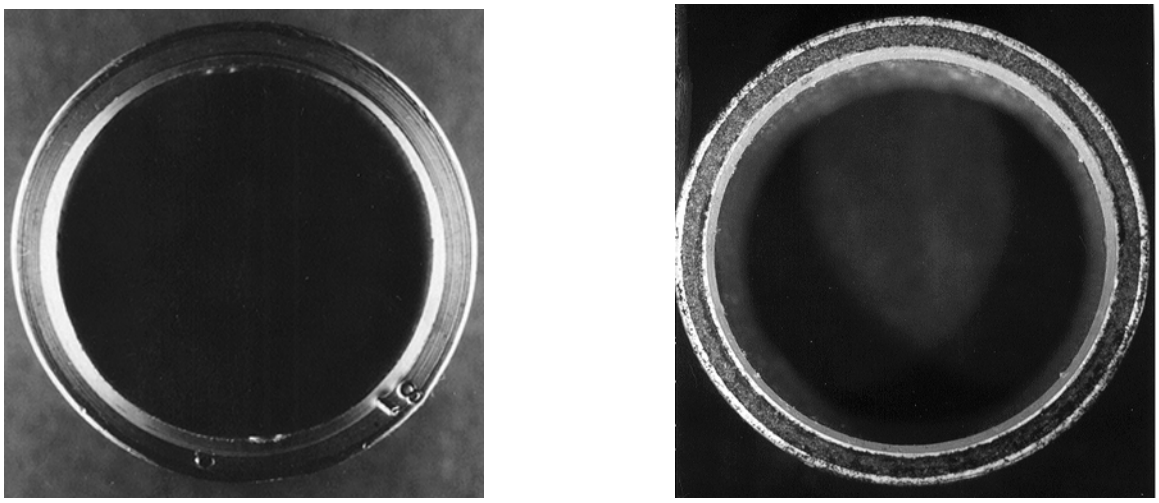

(a) **(b)**

Figure 6 (a) As Received Fuel Tube showing Capsule Aluminum 8001 Cladding and Aluminum 18 wt% Uranium Core (b) Corroded Specimen in a Initial 100% R. H. Water Vapor and Nitric Acid at 150°C for 12-Month Exposure

For each of the aforementioned gases, the diffusion coefficient of the species has been measured or estimated. However the trapping/detrapping energies were not easily calculable in the near term. Hence, until definitive models are developed and calculations completed, the release fraction of gases were assumed to be 30%, which is consistent with that used for commercial SNF.

A simple diffusion model may be applied to conservatively estimate the release of gas from Al-SNF. The model for diffusion out of a slab [19] is adopted as a preliminary model for the release of gaseous and volatile species from a fully-exposed fuel plate. The fraction of gas remaining in a slab is given as:

$$\frac{C(t)}{C_o} = \frac{8}{\pi^2}\sum_{j=0}^{\infty}\frac{1}{(2j+1)^2}\exp(-[\frac{(2j+1)\pi}{h}]^2 Dt)$$

where C(t) is the average concentration at time t remaining in a slab of material of thickness h that had an initial gas concentration of Co. D is the diffusion coefficient. Trapping of the gas species is typically considered through a reduction in the diffusion coefficient.

Assuming no trapping of gas, an evaluation is made for Xe release using this model. The diffusivity of Xe in aluminum at 200°C is 2.8E-13 cm^2/sec [20]. Using the fuel meat thickness of 0.05 cm, approximately 85% of the species would be retained in a de-clad fuel material. A similar calculation for tritium using a value of 10^{-6} cm^2/sec for tritium diffusivity at 200°C

reveals that essentially all of the tritium may be released. This however is contrary to SRS experience (wherein tritium is not released until >400°C) and is consistent with the assumed gaseous release of tritium from commercial SNF wherein a value of 30% is assumed.

The fractional release of iodine has been experimentally shown to be $<10^{-6}$ at temperatures <550°C [21]. Also, literature shows that there is no measurable release of Krypton from Al-U alloys at <600°C [22]. These results are consistent with the understanding that species are not released until the solid reaches a temperature of the species boiling point [23].

Therefore, taking the gas release fraction for breached fuel to be 0.3 for normal conditions of transport and 1.0 for accident conditions of transport is very conservative.

Volatile Release

The volatile release considered in this analysis includes Cs, Sr, and Rb. The melting point of Cs is 28°C and the vapor pressure is 6E-1 atm at 600°C. Both strontium and rubidium have a higher melting point and a higher vapor pressure than cesium. Hence, cesium is expected to dominate the release of volatiles. The fractional release of volatiles is estimated at <1E-6 based on experimental data on the release of fission products during fuel melting experiments. Those volatiles that occupy the volume fraction of fuel meat that is release as fines is also included in the fines calculation.

The release of fission product gases and volatiles at high temperatures (> 300°C), including fuel melt down, from clad uranium-aluminum fuel plates was studied experimentally [21]. The fuel consisted of uranium enriched to 40% and irradiated in the Oak Ridge Reactor to 60% burnup. The equipment was designed to trap and measure very small traces of Xe and I and Cs. The experiment showed that fission product gases and volatiles are released in three stages as the temperature is elevated. The release of fission products at temperatures below 550°C was observed to be negligible ($< 10^{-6}$ of the fission product inventory of each specie) [21].

Two heating tests on segments of irradiated aluminum-based fuel that has been de-clad have been recently completed for SRS at ANL [22]. No radionuclide release was detected from segments of either U_3Si_2-Al or UAl_x-Al during furnace tests at 275°C for times up to four months. In the first test, a segment of fuel element irradiated in the Oak Ridge reactor was heated at 275°C for 30 days. The fuel was a dispersion of U_3Si_2 (19.8% enriched) particles in an aluminum matrix clad with 6061-T6 aluminum. Average burnup was 51.4%. The area of fuel exposed to air in the test chamber was 0.6 cm^2. In the second test, the fuel element segment was a dispersion of UAl_x particles (19.8% enriched) in aluminum clad with 6061-T6 aluminum. The fuel element had been irradiated in the Oak Ridge reactor to an average burnup of 66.5%. The area of fuel exposed to air in the test chamber was 0.5 cm^2. The release of gases and volatile fission products were analyzed through both mass spectrometer and analysis of collector plates. There was no release of gas or volatile fission products in either test nor were there any significant changes in fuel microstructure, core-clad interface, or surface oxide thickness detectable by optical microscopy (see Figure 7).

Basis for Crud Source Term

Aluminum spent fuel do not acquire crud in the same manner as commercial SNF. The surface activity of Al-SNF is primarily a result of storage in radioactively contaminated water. The surface activity is estimated from "sip" data. Radioactivity releases from fuel or from contaminated surfaces into water can be measured directly by performing a "sip" test. The test is performed by measuring the activity concentration in a specified volume of water before and after the material "rests" in the water for a specified period.

Sip data taken from onsite fuel shipments was used to develop the basis of the crud source term and its A_2 value for U-Al alloy fuel. Onsite fuel shipments are made in water-filled fuel casks. Sip data taken from onsite shipments was compared to sip data taken from offsite shipments (dry casks) received at SRS Receiving Basin for Off-site Fuels over the last 2 years. Data for fuel shipments in wet environments resulted in sip values 2 to 3 orders of magnitude greater than for dry shipments. For conservatism wet shipment sip data is used to develop the basis for releasable source term associated with U-Al alloy fuel crud.

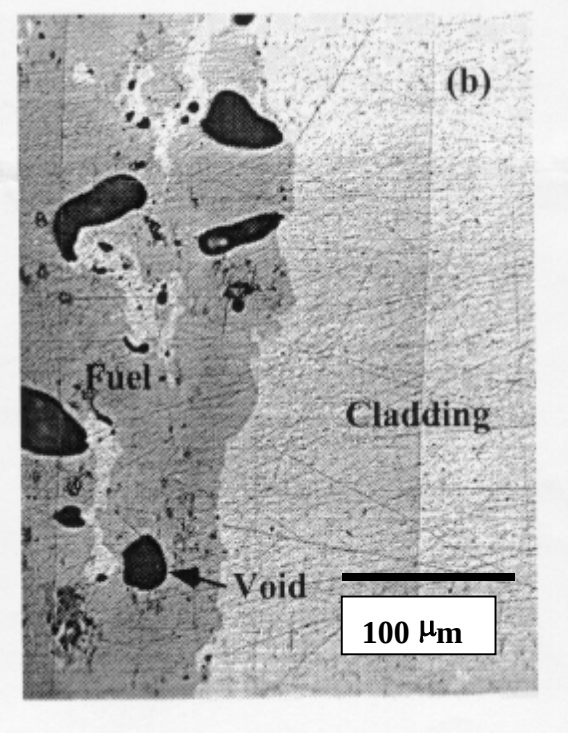

Figure 7 Microstructure of UAl_x-Al Fuel Core at Cladding Interface following 66.5% Burn-up plus 4 Months at 275°C. (Optical micrograph courtesy of A. B. Cohen, Argonne National Laboratory)

Worst case sip results associated with onsite data for MURR fuel were averaged. The source term value represented in dpm/ml, was converted to Ci/cm^2 for a single Al-U SNF assembly and compared to the NRC LWR crud source. LWR crud source term is provided in ANSI N14.5.

Converting the source term value of dpm/ml to Ci/ml and multiplying the resultant dose per volume by the cask volume and dividing by assembly surface area results in the desired dose per area (Ci/cm^2). The calculated value of 1.39E-7 Ci/cm^2 is used in the containment analysis.

The A_2 value used by the NRC for LWR fuel is based on Cobalt and an A_2 value of 10.8 Ci. Gamma spectrography taken on sip samples from SRS basin water was used to develop an effective A_2 value for the crud. The calculated A2 value is 0.270 Ci. The major contributor to the A_2 quantity is Cs-137. It is assumed that the basin level isotope activities are proportional to cask activity levels.

Calculation of source term in the described manner includes several levels of conservatism. The surface area used was 25% of the actual surface area of a single assembly. The total curie content in the cask resulted from 12 fuel assemblies but only one is used for calculation of surface area contamination. Further conservatism is introduced in the use of wet shipment data for dry shipment calculation.

The figure below shows the results for the total exposed fuel surface area as a function of the leakage rate of the cask. For example, if the leak rate of the cask is $1x10^{-5}$ std cm^3/s or less, the cask can be fully loaded with breached fuel and that the total exposed surface area can be at least 250 cm^2.

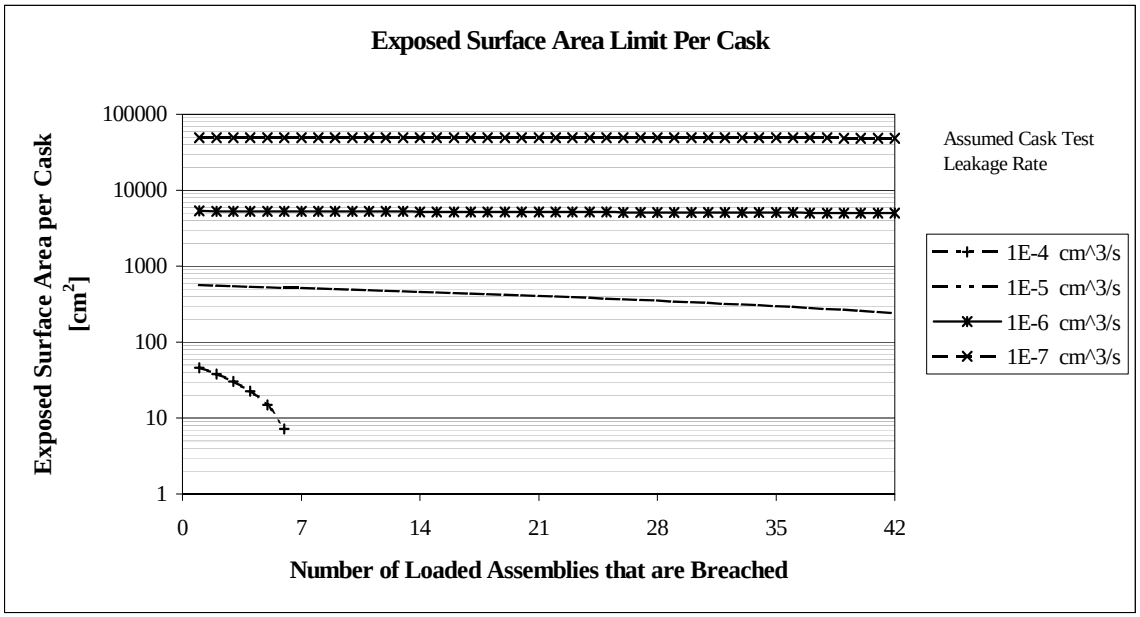

Figure 8 **Exposed Surface Area Limit per Cask as a Function of Cask Leakage Rate and Number of Breached Assemblies.**

References

1. "Packaging and Transportation of Radioactive Material," **10CFR71**.
2. "American national Standard for Radioactive materials – Leakage Tests on Packages for Shipment," **ANSI N14.5-1987**.

3. "Containment Analysis for Type B Packages Used to Transport Various Contents," **NUREG/CR-6487**.
4. "Safety Analysis Document" for Example Cask #1.
5. "Safety Analysis Document" for Example Cask #2.
6. "Characterization of FRR SNF in Basin and Dry Storage Systems," Peggy Brooks and Robert L. Sindelar, presented at the Third Topical Meeting on DOE Spent Nuclear Fuel and Fissile Material Management and published in the proceedings, American Nuclear Society, Charleston, SC, September 1998.
7. **SFS-RSE-970167**, "Proposed New Criteria for Acceptance of Al-SNF for SRS Basin Storage (U)," February 11, 1998.
8. "Radioactivity Release from Aluminum-Based Spent Nuclear Fuel in Basin Storage," R. L. Sindelar, S. D. Burk, and J. P. Howell, presented at the Third Topical Meeting on DOE Spent Nuclear Fuel and Fissile Material Management and published in the proceedings, American Nuclear Society, Charleston, SC, September 1998.
9. M. R. Louthan, Jr., et al, "Corrosion of Aluminum-Clad Fuel and Target Elements: the Importance of Oxide Films and Irradiation History," in the Proceedings of the Embedded Topical Meeting on DOE Spent Nuclear Fuel and Fissile Material Management, American Nuclear Society: La Grange Park, Illinois, 1996, pp. 57-61.
10. G. T. Chandler, R. L. Sindelar, and P. S. Lam, "Evaluation of Water Chemistry on the Pitting Susceptibility of Aluminum," CORROSION/97, Paper No. 104, National Association of Corrosion Engineers, International, Houston, TX, 1997.
11. ASM Handbook, Volume 13 Corrosion.
12. Verbal Communication Dr. Jose Perrotta, IPEN, Brazil to SRTC, September 1998.
13. "Evaluation of Test Methodologies for Dissolution and Corrosion of Al-SNF," B. J. Wiersma, J. I. Mickalonis, and M. R. Louthan, Jr., presented at the Third Topical Meeting on DOE Spent Nuclear Fuel and Fissile Material Management and published in the proceedings, American Nuclear Society, Charleston, SC, September 1998.
14. J. E. Draley, S. Mori, and R. E. Loess, J. Electrochemical Soc. 114 (1967) p. 353.
15. **SRT-MTS-96-2041**, "TRIP REPORT: Characterization of IEA-R1 Spent Nuclear Fuels at the IPEN, Sao Paulo, Brazil, July 22 – July 31, 1996 (U), R. L. Sindelar, H. B. Peacock, Jr., J. P. Howell, S. D. Burke, and A. S. Busby, Westinghouse Savannah River Co., Savannah River Technology Center.
16. P. R. Openshaw and L. L. Shreir, "Oxidation of Uranium-Aluminum Intermetallic Compounds," Corrosion Science, 1963, Vol. 3 pp. 217 to 237.
17. "Vapor Corrosion of Aluminum Cladding Alloy," P. S. Lam, R. L. Sindelar, and H. B. Peacock, Jr., presented at the Third Topical Meeting on DOE Spent Nuclear Fuel and Fissile Material Management and published in the proceedings, American Nuclear Society, Charleston, SC, September 1998.
18. Steam Tables.
19. P. Shewmon, Diffusion in Solids, The Minerals, Metals, & Materials Society, 1989.
20. F.H. Mohlbier, ed. John Askill, Tracer Diffusion Data for Metals and Alloys.
21. T. Shibata, T. Tamai, M. Hayashi, J. C. Posey, and J. L. Snelgrove, "Release of Fission Products from Irradiated Aluminide Fuel at High Temperatures," Nuclear Science and Engineering, 87 (1984) pp. 405-417.
22. M. B. Reynolds, "Fission Gas Behavior in the Uranium-Aluminum System," Nuclear Science and Engineering, 3 (1958) pp. 428-434.

23. “Fission Product Release from Spent Nuclear Fuel During Melting,” J. P. Howell and J. F. Zino, presented at the Third Topical Meeting on DOE Spent Nuclear Fuel and Fissile Material Management and published in the proceedings, American Nuclear Society, Charleston, SC, September 1998.
24. Interlaboratory Memo from Argonne National Laboratory to SRTC, SRTC Fission Product Collection Test 96-2, August 20, 1997.